Mesoscale Aspects of the Downshear Reformation of a Tropical Cyclone

JOHN MOLINARI

Department of Earth and Atmospheric Sciences, The University at Albany, State University of New York, Albany, New York

PETER DODGE

NOAA/AOML/Hurricane Research Division, Miami, Florida

DAVID VOLLARO AND KRISTEN L. CORBOSIERO

Department of Earth and Atmospheric Sciences, The University at Albany, State University of New York, Albany, New York

FRANK MARKS JR.

NOAA/AOML/Hurricane Research Division, Miami, Florida

(Manuscript received 11 November 2003, in final form 12 August 2004)

ABSTRACT

The downshear reformation of Tropical Storm Gabrielle (2001) was investigated using radar reflectivity and lightning data that were nearly continuous in time, as well as frequent aircraft reconnaissance flights. Initially the storm was a marginal tropical storm in an environment with strong 850–200-hPa vertical wind shear of 12–13 m s^{-1} and an approaching upper tropospheric trough. Both the observed outflow and an adiabatic balance model calculation showed that the radial-vertical circulation increased with time as the trough approached. Convection was highly asymmetric, with almost all radar return located in one quadrant left of downshear in the storm. Reconnaissance data show that an intense mesovortex formed downshear of the original center. This vortex was located just south of, rather than within, a strong downshear-left lightning outbreak, consistent with tilting of the horizontal vorticity associated with the vertical wind shear. The downshear mesovortex contained a 972-hPa minimum central pressure, 20 hPa lower than minimum pressure in the original vortex just 3 h earlier. The mesovortex became the new center of the storm, but weakened somewhat prior to landfall. It is argued that dry air carried around the storm from the region of upshear subsidence, as well as the direct effects of the shear, prevented the reformed vortex from continuing to intensify.

Despite the subsequent weakening of the reformed center, it reached land with greater intensity than the original center. It is argued that this intensification process was set into motion by the vertical wind shear in the presence of an environment with upward motion forced by the upper tropospheric trough. In addition, the new center formed much closer to the coast and made landfall much earlier than predicted. Such vertical-shear-induced intensity and track fluctuations are important to understand, especially in storms approaching the coast.

1. Introduction

Vertical wind shear has been shown to be inversely correlated with tropical cyclone frequency (e.g., Gray 1968). In two operational methods for predicting tropical cyclone intensity, the Statistical Hurricane Intensity Prediction Scheme (SHIPS) model (DeMaria and Kaplan 1994; DeMaria et al. 2005) and the Coupled Hurricane Intensity Prediction System (CHIPS) dynamical model (Emanuel et al. 2004), vertical wind shear appears as purely a negative factor that, other factors being equal, increases in influence monotonically with increasing shear. In SHIPS a minor exception occurs at high latitudes, where nonzero shear can lead to prediction of increased intensity, likely reflecting baroclinically aided development (M. DeMaria 2003, personal communication). Numerical studies with full-physics

Corresponding author address: John Molinari, Dept. of Earth and Atmospheric Sciences, The University at Albany, State University of New York, Albany, NY 12222.
E-mail: molinari@atmos.albany.edu

mesoscale models show that the imposition of uniform environmental vertical wind shear always results in a weaker vortex (Wang and Holland 1996; DeMaria 1996), although the response may not be immediate (Frank and Ritchie 2001). The net amount of weakening in these idealized studies is proportional to the magnitude of vertical wind shear. It has been argued (Zehr 1992) that when vertical wind shear over the depth of the troposphere exceeds 12–13 m s^{-1}, tropical cyclone development simply does not occur. In none of these studies can it be said that the presence of vertical wind shear can produce a stronger disturbance.

Vertical shear imposed on an existing vortex creates azimuthal asymmetries in vertical motion, with maximum upward motion and enhanced convection downshear or left of downshear. This asymmetry is remarkably similar whether the vortex is present only at midlevels in association with mesoscale convective systems over land (Trier et al. 2000a,b) or in tropospheric-deep tropical cyclone vortices over water (Marks et al. 1992; Franklin et al. 1993; Wang and Holland 1996; Reasor et al. 2000; Frank and Ritchie 2001; Black et al. 2002; Braun 2002; Corbosiero and Molinari 2002, 2003). Enhanced asymmetric convection creates localized cyclonic vorticity, sometimes near the surface (Hendricks et al. 2004) and sometimes at middle levels (e.g., Ritchie and Holland 1997). The interaction of the primary vortex with these convectively generated vorticity maxima can produce intensification of the primary vortex as it absorbs the asymmetric vorticity (Ritchie and Holland 1997; Simpson et al. 1997; Montgomery and Enagonio 1998; Möller and Montgomery 2000). Reasor and Montgomery (2001) argued that if downshear convergence and enhanced convection were larger than could be produced by symmetric mechanisms alone, intensification of a storm could be accelerated by the presence of vertical wind shear. By this reasoning, vertical wind shear could initiate a process that ultimately produces a more intense storm than would have occurred with zero vertical wind shear. Because the symmetric circulation generally increases with storm intensity, this possibility is most likely during the early asymmetric stages of tropical cyclones.

Guinn and Schubert (1993) and Enagonio and Montgomery (2001) showed results of simulations in which the asymmetric vorticity was much stronger than that of the original vortex. Under these circumstances the new vortex absorbed the old and produced a much stronger vortex than existed initially. Molinari et al. (2004) argued that during its early stages, Hurricane Danny (1997) experienced downshear reformation of the center in the presence of moderate 850–200-hPa vertical wind shear of 5–11 m s^{-1}. They provided evidence that the reformed vortex was stronger than the original vortex, and concluded that vertical wind shear played a contributory role in the intensification process.

Tropical cyclogenesis also occurs in the presence of vertical wind shear associated with the approach of an upper tropospheric trough. Bracken and Bosart (2000) found that the composited environment around forming tropical depressions in the western Atlantic contained an upper tropospheric trough to the northwest of the center and deep-layer vertical wind shear over the center of 10 m s^{-1}. Such troughs can produce an enhanced radial-vertical circulation that offsets the influence of increasing vertical wind shear (e.g., Hanley et al. 2001). Bosart and Bartlo (1991) described the formation of Hurricane Diana (1984) during a trough interaction. Davis and Bosart (2001, 2002) and Hendricks et al. (2004) simulated the development of Hurricane Diana. In the absence of the upper tropospheric trough, no tropical cyclone development occurred in the simulation (Davis and Bosart 2002). When the trough was present, they found that vortex interactions like those described above played an important role in the development.

The studies above raise the possibility that moderate vertical wind shear can set off a sequence of events that produces a stronger vortex. The process appears to be aided by the approach of an upper tropospheric trough that, in addition to supplying vertical wind shear, produces additional upward motion within the storm. In the current paper, the role of vertical wind shear will be examined in a storm (Tropical Storm Gabrielle in the Gulf of Mexico in 2001) in which several factors noted above are present: vertical wind shear magnitude exceeding 10 m s^{-1}, highly asymmetric convection, interaction with an upper tropospheric trough, and an apparent downshear redevelopment. Unlike Hurricane Danny in the study by Molinari et al. (2004), Gabrielle was close enough to the coast to be within range of a coastal radar during its intensification. In addition, U.S. Air Force reconnaissance aircraft sampled a remarkable mesovortex near the time of strongest vertical wind shear. This vortex contained a minimum surface pressure of 972 hPa, 20 hPa lower than that in the storm just 3 h before. The mesoscale evolution of Tropical Storm Gabrielle will be examined and contrasted with that of Hurricane Danny. It is of primary interest to further investigate the complex manner in which vertical wind shear influences the early stages of tropical cyclogenesis.

2. Data sources

The primary data sources for this study are (i) cloud-to-ground lightning locations from the National Light-

ning Detection Network (NLDN); (ii) aircraft reconnaissance data from flights by the U.S. Air Force; (iii) gridded analyses from the European Centre for Medium-Range Weather Forecasts (ECMWF); and (iv) Weather Surveillance Radar-1988 Doppler (WSR-88D) data from the Tampa, Florida, coastal radar. The first three sources have been described in detail by Molinari et al. (2004) and will be discussed only briefly.

The original NLDN is described by Orville (1991). The upgraded network present during Tropical Storm Gabrielle is described by Cummins et al. (1998). Idone et al. (1998a,b) describe the gains in accuracy achieved by the upgraded network. Tropical Storm Gabrielle was well within the 400–600-km nominal range of the network during the period of interest in this study. The interpretation of lightning in hurricanes is discussed by Black and Hallett (1999), Molinari et al. (1999), Cecil and Zipser (2002), and Molinari et al. (2004). One aspect of the interpretation is straightforward. If a dense outbreak of negative flashes (those bringing negative charge to ground) occurs over a small region, it is likely to be accompanied by strong upward motion just above the melting level (Zipser and Lutz 1994; Baker et al. 1999). Mass continuity arguments require strong convergence below, which can create rapid intensification when it occurs in a disturbance that already contains large vorticity.

Aircraft reconnaissance data in this study were collected at or near the 1.5- or 3-km levels (about 850 and 700 hPa, respectively). The data are stored every 10 s (representing approximately 1.15-km horizontal resolution). In addition to wind observations, "D values" from the flights will be shown. These represent deviations of pressure altitude from its standard atmosphere value. Horizontal gradients of D values are identical to height gradients on the local pressure surface. Temperature and moisture data from these flights must be viewed with caution because of sensor wetting problems that can produce spuriously low temperature readings, especially in cloudy layers (Eastin et al. 2002). The Air Force reconnaissance data have the great advantages of being nearly continuous in time (in a storm near landfall) and containing repeated searches for the lower tropospheric center. Such data are particularly valuable during the formative stages of a strongly sheared storm. No flights were made by National Oceanic and Atmospheric Administration (NOAA) research aircraft during the period of interest in this study.

Storm center positions every 6 h were obtained from the best-track dataset assembled by the Tropical Prediction Center. Gridded analyses from ECMWF will be used to determine vertical wind shear between 850 and 200 hPa averaged over 500 km of radius, and to show the structure of the storm environment. Corbosiero and Molinari (2002) argued that the vertical wind shear estimates are accurate to within 1–2 m s^{-1}.

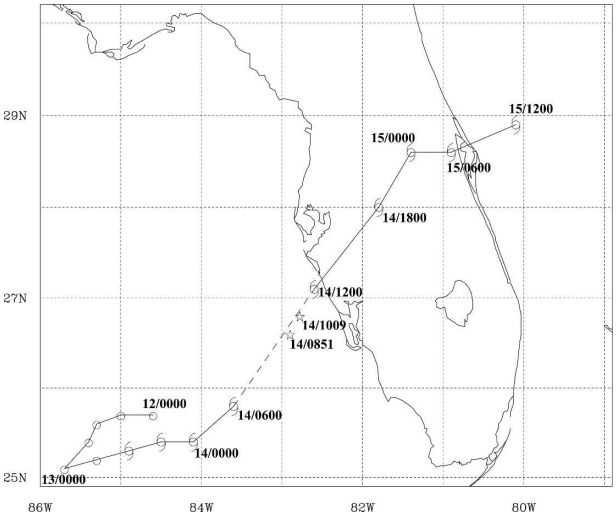

FIG. 1. Best track of Tropical Storm Gabrielle. Times are labeled every 24 h prior to 14 Sep, and every 6 h otherwise. The stars show intermediate storm center positions determined by reconnaissance aircraft.

The Tampa WSR-88D radar collected volume scans every 6 min during Tropical Storm Gabrielle. These data are archived at the National Climatic Data Center. The maximum range from the radar for reflectivity data is 450 km, but incomplete beam filling and elevation of the beam usually limit useful reflectivity data in hurricanes to within 350 km of the radar. The range correction applied to the reflectivity is constant beyond 230 km. The maximum range of recorded Doppler velocity data is 230 km, but the maximum unambiguous range is usually 150–180 km, depending on the choice of pulse repetition frequency (Crum et al. 1993). Data beyond that range are often masked when there is strong echo closer to the radar. During the period of this study the center of circulation was beyond the effective Doppler range, and only reflectivity data will be used.

3. Storm history and large-scale environment

The history of Tropical Storm Gabrielle is given by Lawrence and Blake (2002). The Tropical Storm designation will be used in this paper because the storm did not become a hurricane until after the period of interest in this study. The track of the storm through 1200 UTC 15 September 2001 is shown in Fig. 1. The storm was declared a tropical depression at 1800 UTC 11 September after developing from a midlevel nontropical low

pressure area. Steering currents were initially weak, and the storm moved in a small cyclonic loop while slowly intensifying to a tropical storm at 1200 UTC 13 September. Musgrave et al. (2004) investigated this early development period of Gabrielle, which resembled that of Hurricane Diana discussed in the introduction. An upper-tropospheric trough approached Tropical Storm Gabrielle early on 14 September. The storm moved northeastward and intensified from 25 to 30 m s^{-1} maximum surface wind speed over the 6 h prior to landfall in Florida near 1200 UTC 14 September. Figure 1 shows two additional center positions during this period based on reconnaissance aircraft estimates. The first of these, at 0851 UTC 14 September, represents the location of the 972-hPa mesovortex sampled by the aircraft. The 12-h period before landfall near 1200 UTC 14 September is of primary interest in this study. Knupp et al. (2006) have examined the structure and evolution of the storm at and after landfall.

Table 1 gives the direction and speed of storm motion for three 6-h periods on 14 September based on the best-track positions in Fig. 1. In addition, the mean flow between 1000 and 200 hPa, averaged over 500 km of radius, is provided for the same time periods. Tropospheric mean flow and storm motion differed by less than 1 m s^{-1} during the periods before 0600 and after 1200 UTC 14 September. Between 0600 and 1200 UTC, however, the best-track positions indicate a storm motion nearly twice that of the mean flow, an unlikely event. During this time convection was asymmetric, with almost all high clouds east and northeast of the center, and forecasters argued in real time that the storm might have reformed under the most active convection. The dramatic difference between mean flow and storm motion shown in Table 1 supports this interpretation.

Table 2 gives the vertical wind shear between 850 and 200 hPa every 6 h on 14 September 2001, as well as minimum pressure and maximum surface winds in the storm for the same times. Vertical shear was large from the west early in the period, reaching 13 m s^{-1} at 0600 UTC, and remained large from the west-southwest at 12 m s^{-1} at 1200 UTC. The intensification of the storm during this period makes the study of the influences of wind shear especially relevant. Tables 1 and 2 show that the storm motion vector was oriented almost exactly 45° counterclockwise from the vertical wind shear vector, consistent with the results from a large number of sheared storms given by Corbosiero and Molinari (2003).

TABLE 1. Tropospheric mean flow, averaged between 1000 and 200 hPa and over 500 km of radius, vs motion of Tropical Storm Gabrielle using best-track positions, during the times of interest in this study. Values were calculated using gridded analyses from the ECMWF.

Time	Mean flow	Storm motion
0000–0600 UTC 14 Sep	229° at 3.3 m s^{-1}	228° at 3.1 m s^{-1}
0600–1200 UTC 14 Sep	216° at 4.3 m s^{-1}	215° at 8.1 m s^{-1}
1200–1800 UTC 14 Sep	211° at 5.1 m s^{-1}	218° at 5.9 m s^{-1}

TABLE 2. (middle) Vertical wind shear between 850 and 200 hPa, averaged within 500 km of the center of Tropical Storm Gabrielle, calculated using gridded analyses from the ECMWF. (right) minimum central pressure and maximum surface winds in the storm during the times of interest in this study, taken from the best-track data determined by the Tropical Prediction Center.

Time	Vertical wind shear	Min pressure, max wind
0000 UTC 14 Sep	276° at 11.8 m s^{-1}	997 hPa, 22.5 m s^{-1}
0600 UTC 14 Sep	271° at 13.3 m s^{-1}	992 hPa, 25.0 m s^{-1}
1200 UTC 14 Sep	252° at 12.3 m s^{-1}	983 hPa, 30.0 m s^{-1}
1800 UTC 14 Sep	230° at 16.4 m s^{-1}	994 hPa, 22.5 m s^{-1}

Figure 2 shows potential vorticity fields on the 350-K isentropic surface at 0000 and 1200 UTC 14 September. This surface lies mostly between 175 and 225 hPa, except it approaches 150 hPa in the regions of outflow east of the storm center. It is apparent that a midlatitude trough approached but never reached the tropical storm center on 14 September. The nature of the trough interaction in this case is not a "superposition" (Molinari et al. 1995), but instead a "distant interaction" (Hanley et al. 2001). When superposition occurs, tropical cyclone intensification can be attributed to constructive interference between overlying positive potential vorticity (PV) anomalies (K. Emanuel 1989, personal communication; see also Hoskins 1990; Molinari et al. 1995). In Gabrielle, however, the influence of the trough must be less direct. Shi et al. (1997), Bosart et al. (2000), and Hanley et al. (2001) argued that such interactions produce jets downstream of the tropical cyclone in the upper troposphere, with the tropical cyclone lying beneath the jet entrance region where upward motion is favored. Such a configuration appears in Fig. 2, with a jet northeast of the storm center.

Molinari and Vollaro (1989) investigated trough interactions using radial flux convergence of angular momentum by azimuthal eddies, given by

$$-\frac{1}{r^2}\frac{\partial}{\partial r} r^2 \overline{u_L' v_L'},$$

where u_L and v_L are storm-relative radial and tangential velocity, respectively, and the bar and prime represent azimuthal mean and eddy. Figure 3a shows a radi-

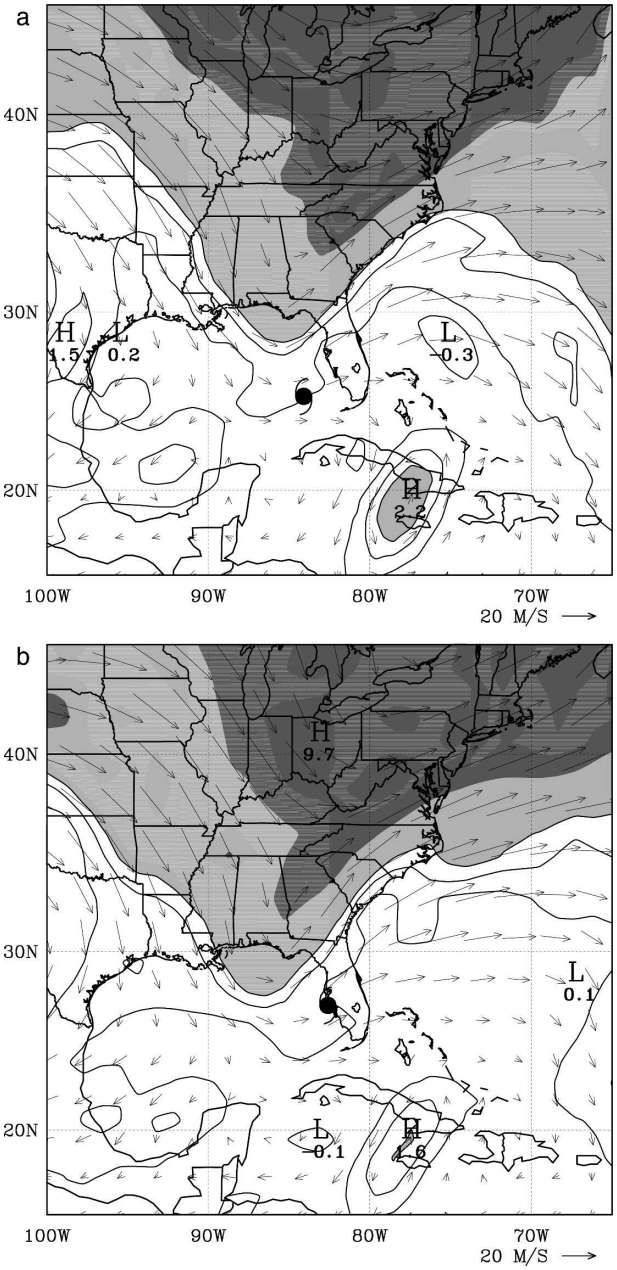

FIG. 2. Potential vorticity and winds on the $\theta = 350$ K surface (upper troposphere) at (a) 0000 and (b) 1200 UTC 14 Sep 2001. Potential vorticity is contoured from 0 to 1.5 potential vorticity units (PVU, where 1 PVU = 1.0×10^{-6} m^2 s^{-1} K kg^{-1}) in increments of 0.5 PVU, and shaded for higher values. The light, moderate, and dark shading regions begin at 1.5, 2.5, and 5 PVU, respectively.

us–time series of the above quantity at 200 hPa in Tropical Storm Gabrielle from 1200 UTC 13 September to 1800 UTC 14 September. It is expressed in units of meters per second per day of spinup of mean tangential velocity. The stronger spinup at 1200 UTC 14 September than at 0000 UTC shown in Fig. 3a reflects

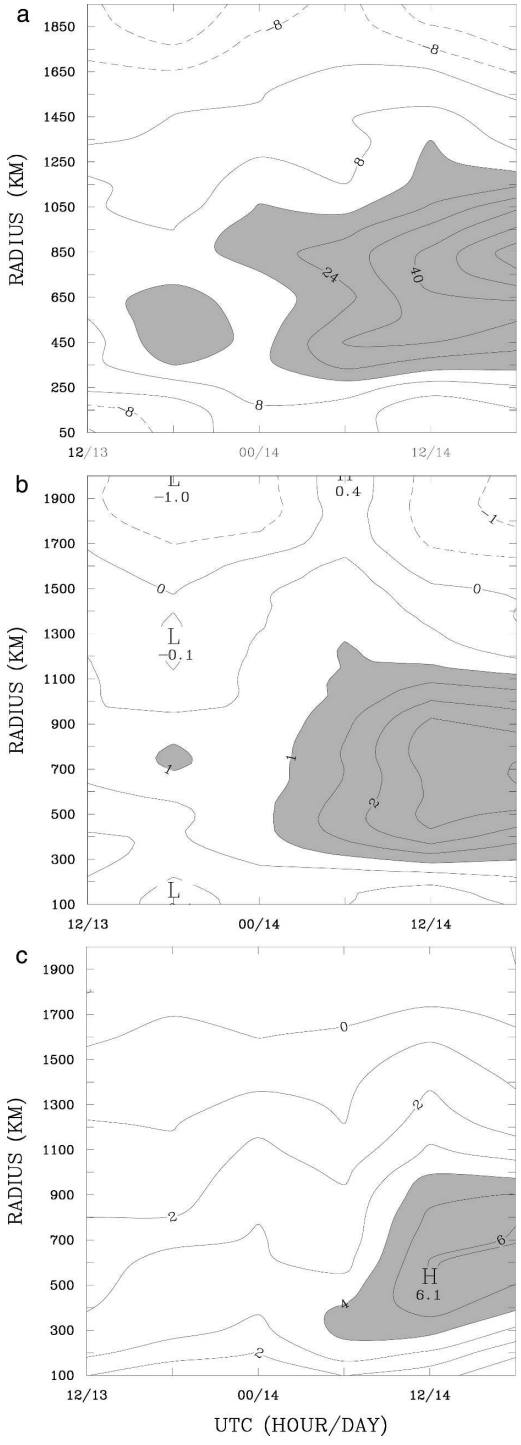

FIG. 3. (a) Radius–time series of the radial convergence of flux of tangential velocity by azimuthal eddies at 200 hPa (see text equation). Contour increment is 8 m s^{-1} day^{-1}, and values greater than 16 m s^{-1} day^{-1} are shaded. (b) As in (a), but for balanced radial velocity at 200 hPa, calculated from the balanced vortex model of Molinari and Vollaro (1990). Contour increment is 0.5 m s^{-1}, and values greater than 1 m s^{-1} are shaded. (c) As in (b), but for observed radial velocity. Contour increment is 1 m s^{-1}, and values greater than 4 m s^{-1} are shaded.

the mutual approach of the trough and the tropical storm shown in Fig. 2. The definition of an active trough interaction used by Hanley et al. (2001) is met during the entire 24-h period ending 1800 UTC 14 September. The value of 200-hPa cyclonic spinup reached 40 m s^{-1} day^{-1} just before the landfall of Tropical Storm Gabrielle, indicative of a strong trough interaction [see Fig. 3 of Hanley et al. (2001) for a typical range of values].

Figure 3b shows the balanced outflow at 200 hPa associated with the trough forcing, calculated using the balanced model of Molinari and Vollaro (1990). This calculation is adiabatic and shows the divergent circulation required to balance the effects of eddy potential temperature and angular momentum fluxes. It is apparent that the dynamical influence of the trough was to enhance upper tropospheric outflow, and thus to enhance upward motion, especially at 0600 and 1200 UTC 14 September. The forcing was even stronger at 1800 UTC, but the storm was over land at that time.

Figure 3c shows the observed radial velocity at 200 hPa. The balanced outflow calculations do not account for the effects of heating, and thus the observed flow is larger than that shown in Fig. 3b. Nevertheless, the time change of the two fields is quite similar; in both, the strongest increase in outflow occurred between 0000 and 1200 UTC 14 September. The evidence supports the conclusion that the increase in radial-vertical circulation on 14 September is associated with the approach of the upper tropospheric trough.

Upper tropospheric potential vorticity maxima also create vertical wind shear over the hurricane [see arguments by Molinari et al. (1998) based on the work of Thorpe (1986)]. Table 2 showed that vertical wind shear was large from the west and west-southwest, consistent with the influence of the upper tropospheric potential vorticity maximum shown in Fig. 2.

Overall, the dynamical environment of Tropical Storm Gabrielle between 0000 and 1200 UTC 14 September was dominated by a midlatitude trough that produced enhanced upward motion within the storm, but also contributed strong vertical wind shear. The mesoscale response to this environment will be addressed in the following section.

4. Mesoscale evolution

Clouds, lightning, and reconnaissance winds

Figure 4 shows the frequency of cloud-to-ground lightning flashes between 25°–28°N and 81°–84°W, which closely resembles the entire region shown in Fig. 5. Almost all the lightning in Tropical Storm Gabrielle between 0000 and 1200 UTC 14 September occurred in this region. Also shown in Fig. 4 is the best-track central pressure, and two additional central pressure observations at the intermediate times shown in Fig. 1. Lightning in this region reached about 100 flashes per hour at 0400 UTC, jumped to over 500 flashes at 0600 UTC,

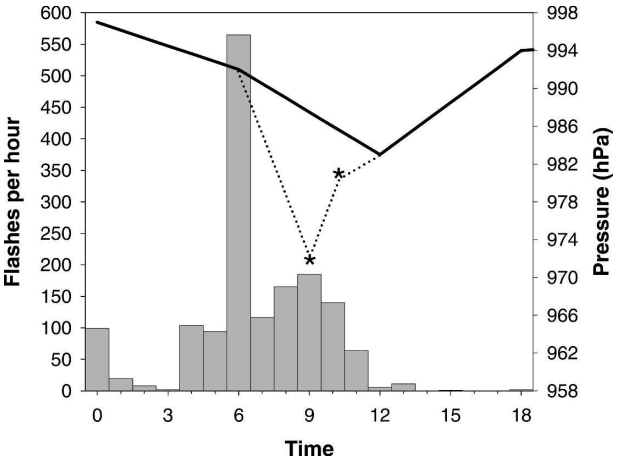

FIG. 4. Hourly time series of the number of cloud-to-ground lightning flashes in the region 25°–28°N, 81°–84°W, plus best-track minimum central pressure (solid) and intermediate minimum pressure values between 0600 and 1200 UTC 14 Sep from aircraft reconnaissance (dotted).

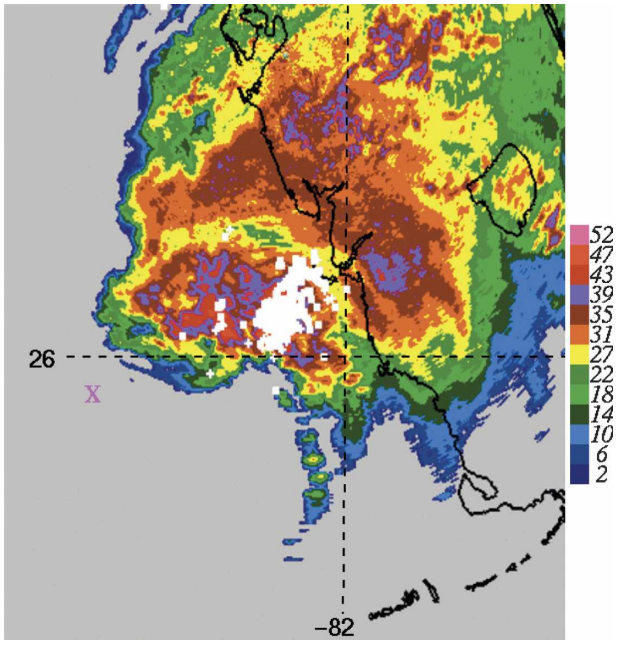

FIG. 5. PPI image from the Tampa radar at 0601 UTC 14 Sep 2001. Reflectivity values (dBZ) are given by the color bar to the right. White dots and plus signs show the locations of cloud-to-ground lightning flashes with negative and positive polarity, respectively, for a 30-min period centered on the time of the image. The magenta X represents the best-track storm center at this time.

and remained above 100 flashes per hour until 1000 UTC. After landfall, lightning sharply decreased in frequency.

The evolution of Tropical Storm Gabrielle will be shown with three sets of fields: infrared Geostationary Operational Environmental Satellite (GOES) images, plan position indicator (PPI) images from the Tampa radar, and cross sections of winds and D value during center crossings by U.S. Air Force aircraft reconnaissance. No satellite image is available at 0600 UTC, during the intense lightning outbreak, because of satellite eclipse. (This phenomenon is described for a geostationary satellite online at www.srh.noaa.gov/ssd/html/goesfaqs.htm.) Only radar reflectivity will be shown at that time. Satellite images will be shown at 0645, 0745, 0845, and 0945 UTC. The last three images lie near aircraft center crossing times at 0741, 0851, and 1007 UTC. Radar images are available every 5 min and will be shown nearest the times that reconnaissance aircraft crossed the center. Lightning will be shown for 1 h centered on the satellite images, because the high cloud tends to represent the cumulative effect of an extended period of convection. Lightning will be shown for only one-half hour centered on the radar images, because the radar images have greater detail and larger time change, and 1 h of lightning deviates too far from the instantaneous detailed reflectivity structure. The cross sections of reconnaissance winds and D values through the storm center will be shown at much higher time resolution than is possible on satellite or radar in order to show important detail near the center. The somewhat circular flight track for the center passage near 1007 UTC (see Fig. 9a) did not allow construction of a reconnaissance data cross section for that time period. The goal of this set of figures is to display as clearly as possible the mesoscale evolution of the storm during the downshear reformation of the center.

Figure 5 shows the Tampa radar image at 0601 UTC, when no satellite image is available. Also displayed is the best-track center position at 0600 UTC (magenta X). Vertical wind shear was from the west at this time (Table 2). It is apparent that the storm was highly asymmetric, with the highest reflectivity and the strong lightning outbreak east-northeast (downshear left) of the center. Although the storm center in Fig. 5 lies on the edge of radar range, it is well within range of the NLDN. Subsequent images will confirm that the lack of convection near the storm core and upshear of the storm center do not relate to attenuation of the radar signal. Figure 5 shows cyclonic bands of heavy precipitation downshear, but no evidence of a center reformation.

Figure 6 shows infrared satellite and radar images at 0645 UTC 14 September. Also shown are lightning locations, aircraft reconnaissance winds at the 1.5-km level, and surface winds. The storm contained a strongly asymmetric cloud field, with high clouds, like the radar reflectivity earlier, almost exclusively downshear and downshear left of the center, which reconnais-

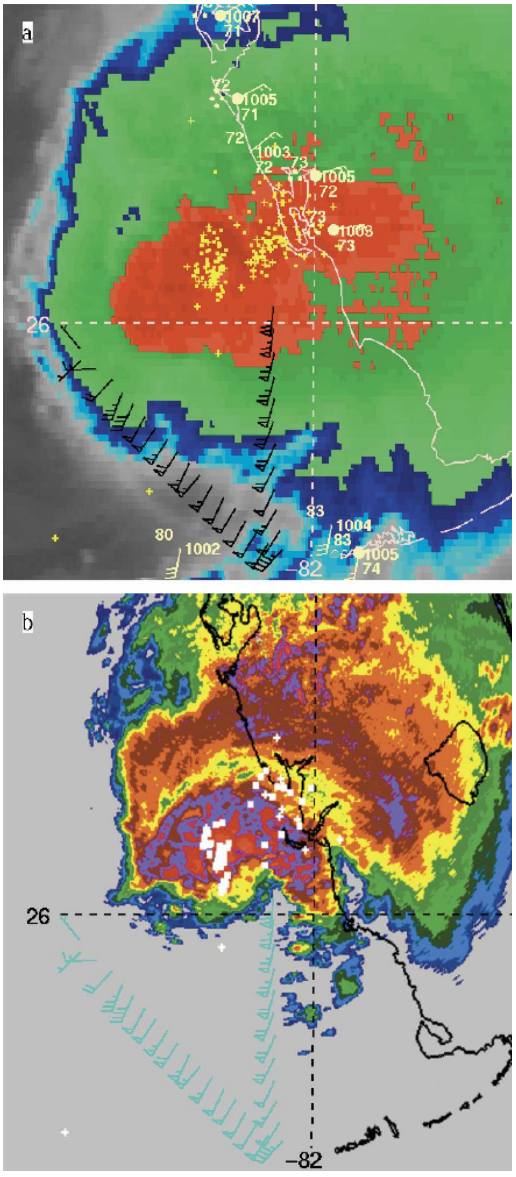

FIG. 6. (a) Infrared satellite image at 0645 UTC 14 Sep. Cyan, blue, green, red, and magenta shading begin at brightness temperatures of 241, 232, 222, 213, and 203 K, respectively. Also shown are aircraft reconnaissance winds (black) at the 1.5-km level for 1 h centered on the image, plotted every 2 min; conventional surface winds (pale yellow) at the time of the image; and lightning locations (yellow dots and plusses) for 1 h centered on the image. (b) Radar reflectivity and lightning as in Fig. 5, but for 0646 UTC 14 Sep. Reconnaissance wind vectors (cyan) are identical to those in (a).

sance winds show was located on the upshear edge of the high clouds. Flight-level wind speeds exceeded 50 kt over a wide area southeast of the center. The lightning outbreak shown in Fig. 5 was weakening, and a second lightning outbreak was developing just to its west.

Figure 6b shows the radar image at 0646 UTC, nearly the same time as the satellite image in Fig. 6a (as noted earlier, lightning plotted on the radar images covers only half the interval of that on the satellite images). The strongest band of high reflectivity appears to be more strongly cyclonically curved compared to the previous hour, but no direct evidence was available to suggest that a new circulation center had formed downshear.

Figures 7a,b show infrared satellite and radar images at 0745 and 0741 UTC, respectively, on 14 September, and Fig. 7c shows higher time resolution winds and D values. The reconnaissance winds again showed the original tropical storm center near the upshear edge of the highest clouds (Fig. 7a) and on the edge of the precipitation (Fig. 7b). A broad cyclonic band of high reflectivity and strong winds was present downshear. Wind speeds fluctuated across the region of strong radar return, producing local maxima and minima in vorticity, as might be expected in a region of strong convection (see, e.g., Hendricks et al. 2004). Total vorticity along the flight track cannot be computed, but shear vorticity of the wind component perpendicular to the flight track gives some indication of where spinup was occurring. The along-track shear vorticity averaged across the lightning outbreak, between the 80-kt wind northeast of the lightning core in Fig. 7a and the 40-kt wind on the southwest side of the lightning, was about 5×10^{-4} s^{-1}. The strongest along-track shear vorticity was not within the heating region, but southwest of that 40-kt wind, where vorticity exceeded 1×10^{-3} s^{-1}.

Figure 7c shows D value and winds from aircraft reconnaissance over a 16-min period (representing about 100 km of distance) just prior to 0800 UTC 14 September. The higher resolution of winds gives a clearer indication of the vorticity structure. The multiple small maxima and minima in D value were consistent with variations in shear vorticity. Nevertheless, it is clear that two primary height minima, associated with two cyclonic circulations, were the dominant features. The height minimum to the southwest is associated with the original center near the upshear edge of the high clouds. The height minimum about 35 km farther northeast appears to represent a second more recently formed center nearer the lightning. These two lows were separated by higher heights and anticyclonic shear of the wind. The distinct height maximum accompanying the anticyclonic shear suggests that the flow is at

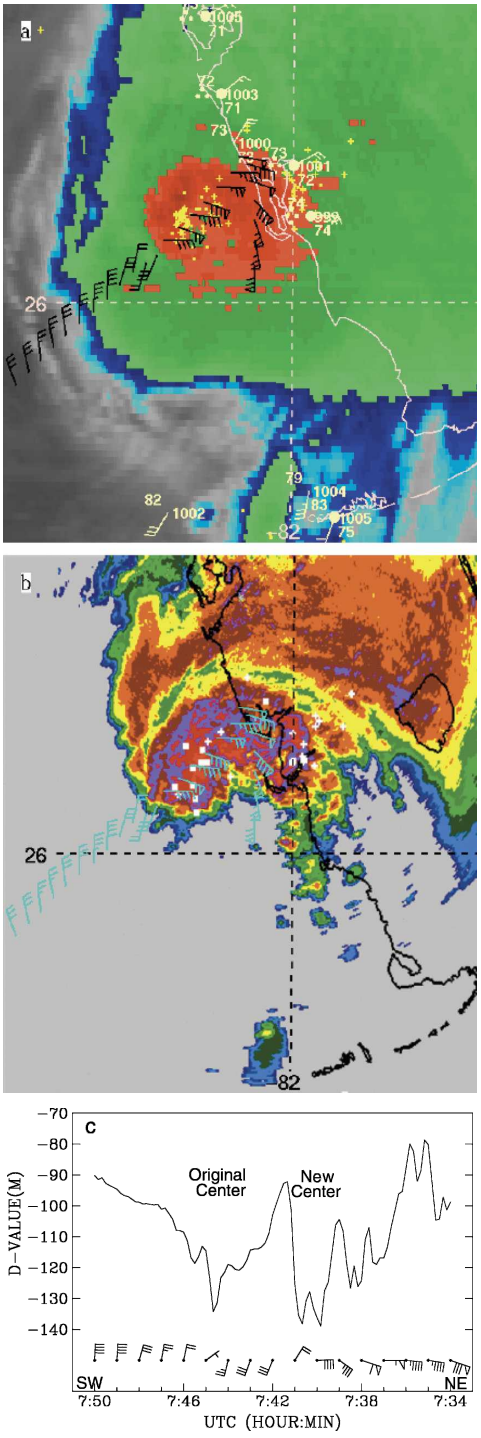

FIG. 7. (a) As in Fig. 6a, but for 0745 UTC 14 Sep. (b) As in Fig. 6b, but for 0741 UTC 14 Sep. (c) D value (deviation of the pressure altitude from standard atmosphere values) plotted every 10 s and winds plotted every minute from 0734 to 0750 UTC 14 Sep, during the period the reconnaissance aircraft was near the original and newly developing centers of Tropical Storm Gabrielle. Time is reversed on the horizontal axis so that NE is to the right. One minute represents approximately 6.9 km, and thus the plot covers a distance of about 100 km approximately centered on the storm.

least partly balanced. The new center occurred at the location noted above in which the along-track shear vorticity exceeded 1×10^{-3} s^{-1}. The winds between 0739 and 0741 UTC in Fig. 7c suggest that the reconnaissance aircraft traveled north of this new center and thus most likely did not sample the lowest heights.

As noted above, the lightning, wind, and pressure distributions in Fig. 7 suggest that the maximum vorticity generation and new center formation occurred at the southern edge of, rather than within, the region of concentrated lightning and high radar reflectivity. Raymond (1992; see also a discussion by Davis and Bosart 2003, p. 2743) noted that when diabatic heating increases along a sloping absolute vorticity vector, potential vorticity is generated. To determine the orientation of the absolute vorticity vector, both vertical and horizontal components of vorticity must be estimated. The vertical component of vorticity across the area of lightning was estimated previously to exceed 1×10^{-3} s^{-1} using reconnaissance winds. If the horizontal component of vorticity is taken to be that associated with the vertical wind shear averaged over the entire storm, it would give positive vorticity around the y axis of 1.2×10^{-3} s^{-1}, that is, consistent with vertical shear from the west of about 12 m s^{-1} over 10 km. The resulting absolute vorticity vector would then tilt toward the north at an angle near 45°. Thus, in a region of diabatic heating, the strongest lower-tropospheric spinup should occur near the southern edge of the lightning outbreak/reflectivity maximum, as was observed. Equivalently, one could estimate the tilting term of the relative vorticity equation: strong upward motion in the region of heating north of the center, and presumably subsidence in the clear air south of the center, would tilt the system-scale horizontal vorticity into the vertical and create spinup between the location of strongest upward and downward motion where the vertical motion gradient was largest. This would again place the developing vortex somewhere south of the maximum heating.

The difficulty with the above reasoning is that it assumes knowledge of the local orientation of the absolute vorticity vector. The vertical vorticity was representative of a local region, but the horizontal vorticity (vertical shear) was taken over a much larger scale, in which the shear of the mean vortex was removed and the local shear was averaged out. It is possible that the local vertical wind shear differs significantly from the area-averaged value. Franklin et al. (2003) showed that wind speed (and thus likely tangential wind) in hurricanes typically decreases upward at the levels sampled by reconnaissance aircraft in this study. That would contribute a local vorticity vector that continuously changes orientation with azimuth. No dropwindsonde data are available to evaluate the local vertical shear in Tropical Storm Gabrielle. It can be said only that the observed spinup of the vortex on the southern edge of the strongest convection is consistent with a northward-tilting absolute vorticity vector. Wang and Holland (1996) used exactly the same reasoning to argue for spinup south of a region of heating in their simulations of hurricane vortices in westerly shear. Davis and Bosart (2003) also used Raymond's (1992) arguments to interpret the relationship between heating and the location of spinup in a numerical simulation of Hurricane Michael (2000).

Figures 8a–c show the same fields as in Fig. 7, but near 0845 UTC 14 September. During these times the aircraft flew at about 3 km, near the 700-hPa level. It appears that the reconnaissance aircraft flew directly through the reformed center at this time. It was at 0850 UTC that reconnaissance estimated a 972-hPa minimum central pressure. This low pressure occurred in the region between the 65- and 15-kt opposing winds at the center of circulation in Figs. 8a,b. A repeat of the previous calculation of shear vorticity around a vertical axis, using those two winds, gives a value of about 4×10^{-3} s^{-1}. The new center was located south-southeast of the lightning outbreak and the highest radar reflectivity (Fig. 8b). Vertical wind shear shifted from west at 0600 UTC to west-southwest at 1200 UTC, thus creating an absolute vorticity vector that leans north-northwest at 1200 UTC. The center location in Fig. 8 thus remained generally consistent with the tilting of system-scale vertical shear. In contrast to previous hours, the lower tropospheric circulation was almost centered under the high clouds.

Figure 8b shows that the reformed center was located at the southwest tip of the strongest rainband in the storm. The reflectivity pattern remained highly asymmetric, with the highest values largely north of the center in the downshear left quadrant. The beginnings of a hooked-shape reflectivity pattern resemble that described in the cloud fields of forming tropical cyclones by Simpson et al. (1997) and Ritchie et al. (2003).

Figure 8c shows the D values and winds during this flight. Rather than the two centers defined just 1 h earlier, a strong localized minimum in D value was present. The magnitude of the minimum D value was smaller than 70 min earlier (Fig. 7c), but this likely relates to the change in flight level from 1.5 to 3 km. The height gradients in Fig. 8c are significantly larger than in the previous hour. Temperature fields in the new center at 0850 UTC (not shown) indicate an 8°C warm anomaly at flight level. Loops of 5-min radar images (not shown) indicate clearly that the vortex

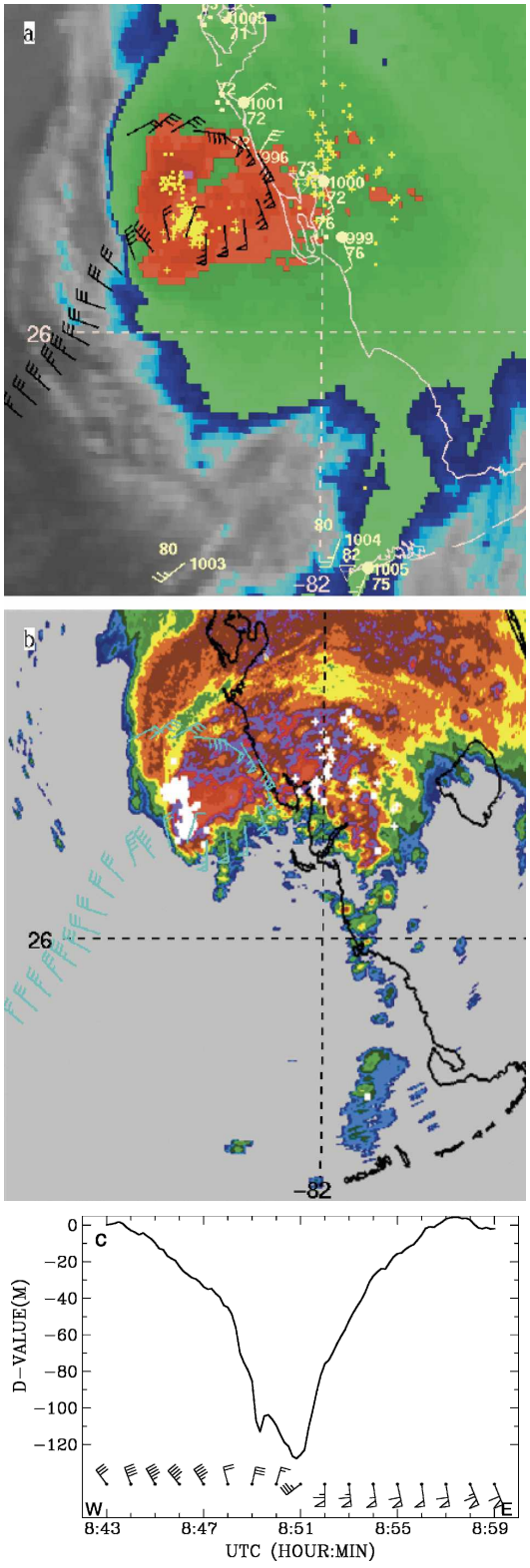

FIG. 8. As in Fig. 7, except the satellite image is for 0845 UTC 14 Sep, radar reflectivity is for 0851 UTC, and the winds and D value from aircraft reconnaissance are at the 3-km level during the period 0843 to 0859 UTC.

shown in Fig. 8 became the center of the storm after this time.

Figure 9 shows satellite and radar images at 0945 and 1007 UTC 14 September, respectively. The highest clouds were northwest of the center. The hooked shape in the radar signature had become more prominent. In addition, lightning was occurring in the upshear left quadrant with respect to the new center, which is unusual (Corbosiero and Molinari 2002). Significant upshear lightning first appeared 1 h before (Fig. 8b). It is speculated that these occurrences reflect the start of a filamentation of the original center by the newly

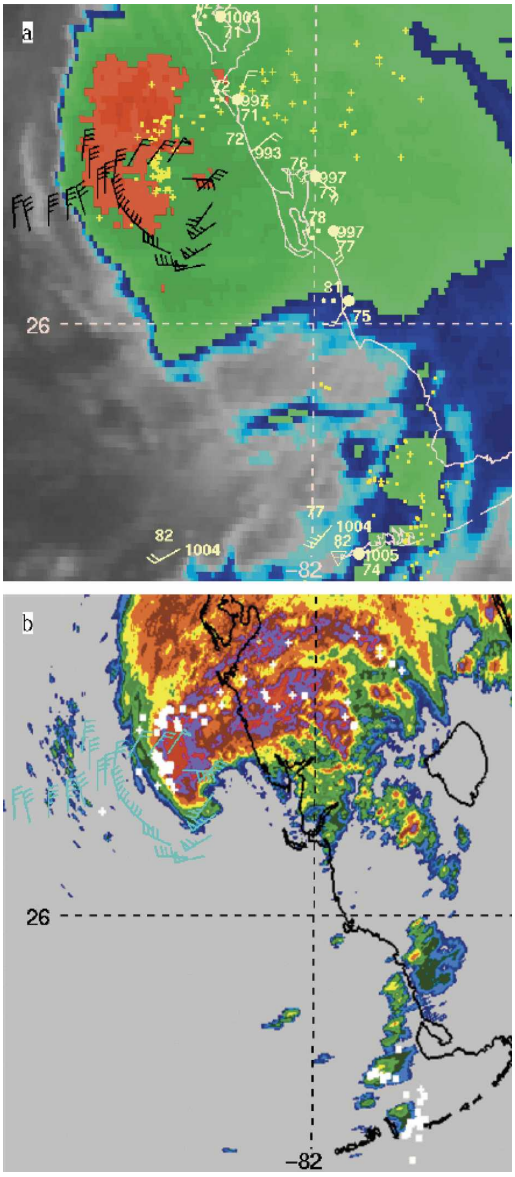

FIG. 9. As in Figs. 7a,b, except the infrared satellite image is at 1015 UTC 14 Sep, the radar reflectivity at 1007 UTC, and the reconnaissance flight level is at 3 km.

formed intense vortex, which could create a crescent-shaped cyclonic vorticity band west and southwest of the new center (e.g., see Enagonio and Montgomery 2001). The development of the prominent hook could represent such an interaction.

Figure 9b also shows a large echo-free region to the west and south of the primary rainband. The most dramatic change from an hour before was the wrapping of the echo-free area around to the east of the center. Central pressure rose 7 hPa from 70 min earlier. Between this hour and landfall, no dramatic change in structure occurred. The storm remained asymmetric in the core and central pressure rose 3 hPa further before landfall. The storm crossed the coast just after 1200 UTC 14 September. The structure and evolution of the storm at and after landfall are described in detail by Knupp et al. (2006). These authors noted a large, shallow pool of rain-cooled air over land as the storm approached the coast. To the extent that this cool air was entrained into the storm core, it may have contributed to the weakening of the intense vortex before landfall.

One striking aspect of the center reformation and subsequent evolution was the continued strongly asymmetric reflectivity in the core. Reflectivity maxima developed upshear from the reformed center, consistent with the structure shown by Willoughby et al. (1984), and also consistent with a downshear left maximum in upward motion caused by vertical shear (Reasor et al. 2004; Trier et al. 2000a,b). The vertical-shear-induced circulations should also produce relative humidity asymmetries, with strongest subsidence and drying upshear right. Figure 10 shows a composite of relative humidity at 700 hPa observed by reconnaissance aircraft between 0800 and 1100 UTC 14 September. The color of the dot along the track indicates the value of humidity as shown. The downshear-left quadrant (northeast of the center) in Fig. 10 shows the highest relative humidity, almost exclusively above 90%. The upshear-left (northwest) quadrant contains fewer points above 90% as one moves cyclonically away from downshear left. As air moved from upshear-left to upshear-right, Fig. 10 shows that relative humidity values generally continued to decrease. Very little sampling was done in the downshear-right (southeast) quadrant, but the few values shown (most of which were collected near 1000 UTC) show the driest air in the storm. This region had the highest winds, and most likely large surface fluxes, just 2 h earlier (Fig. 7b). The relative humidity distribution suggests that air was subsiding as it moved from northwest of the center cyclonically around to the southeast. This reasoning is quite consistent with the reflectivity patterns shown in Figs. 5–9, in which the southeast quadrant showed a decreasing areal coverage of significant reflectivity with time. As the dry air is swept around during intensification, it is likely that further increases in downshear convection would be suppressed, as occurred in Tropical Storm Gabrielle (Fig. 9b). It is hypothesized that in such a strongly sheared storm, this process can act as a governor on storm intensification by preventing an axisymmetric heating field from developing.

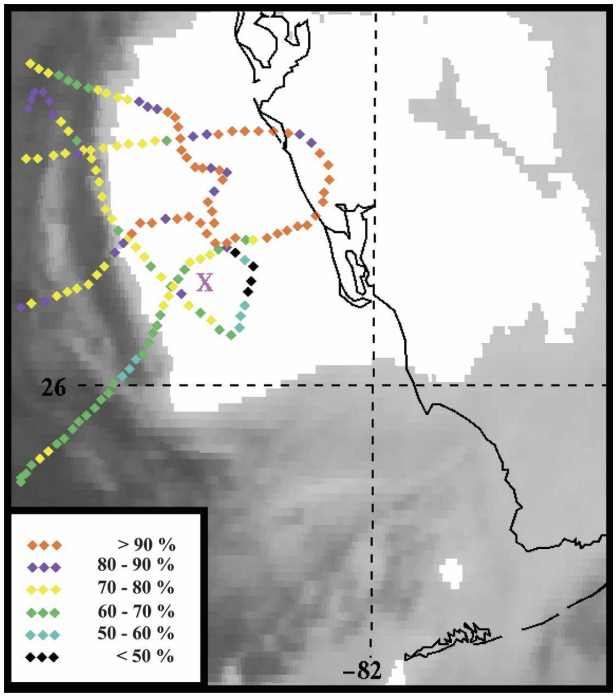

FIG. 10. Color-coded observations of relative humidity from reconnaissance aircraft, plotted with respect to the center, between 0800 and 1130 UTC 14 Sep. Only values from the 3-km level are shown. To aid interpretation, the geography and the infrared image are shown based on the 0945 UTC storm center position (indicated by the magenta X). As a result, the position of each observation is not strictly valid with respect to the geography and high cloud, only with respect to the center of the storm. Vertical wind shear ranged from west just before the period shown to west-southwest just after the period shown, giving the lowest relative humidity downshear right and the highest downshear left.

5. Discussion and conclusions

In the early hours (UTC) of 14 September 2001, weak Tropical Storm Gabrielle experienced 12–13 m s^{-1} vertical wind shear and persistent downshear convection. As an upper trough continued to approach from the north-northwest, a significant convective outbreak developed about 100–120 km from the center and slightly left of directly downshear. This outbreak peaked in the hour centered on 0600 UTC 14 Septem-

ber. Reconnaissance aircraft flights at this time showed a strongly asymmetric storm with a poorly defined center upshear from the active precipitation with a minimum central pressure of 992 hPa. Over the following 3 h, a new circulation center developed just south of the downshear lightning and radar reflectivity maxima. This location adjacent to the diabatic heating maximum was consistent with the generation of potential vorticity by an upward increase in heating along the northward-sloping absolute vorticity vector. The new center was much stronger than the original in terms of vorticity and minimum central pressure, which reached 972 hPa, 20 hPa lower than was measured just 3 h earlier. Radar loops (not shown) indicate clearly that the reformed center took over as the primary circulation in the storm. It was hypothesized that the hook-shaped radar return that developed after the reformation reflected the beginnings of the filamentation of the original vortex. One can conclude that the consequence of the complex interplay among downshear convection, downshear vorticity generation, and interaction of the downshear vortex with the original produced, in the end, a much stronger storm. It seems justified to ascribe this intensification as being put into motion by the presence of substantial vertical wind shear.

The upper tropospheric trough was directly associated with the vertical wind shear, without which no downshear reformation would likely have occurred. In addition, the approach of the trough produced an increase in the mean radial-vertical circulation in the storm (Figs. 3b,c), both during and after the center reformation. As a result, the trough interaction appears to have played an essential role in the intensification of Gabrielle. This reasoning is consistent with the results of Davis and Bosart (2002), who found that Hurricane Diana (1984) did not form in their simulations when the upper trough was removed.

Tropical Storm Gabrielle can be contrasted with Tropical Storm Chantal (2001), which was studied by Heymsfield et al. (2006). Chantal resembled Gabrielle in several aspects: it had 12–13 m s^{-1} of vertical wind shear and repeated outbreaks of intense downshear convection over several days. Chantal, however, had no trough interaction (using the definition of Hanley et al. 2001). Unlike in Gabrielle, no intense downshear vortex formed in the lower troposphere, and Chantal never developed a central pressure lower than 1001 hPa. It is speculated that the lack of a trough interaction in Chantal was a key factor in preventing its development in such a high-shear environment.

Vertical wind shear in excess of 5 m s^{-1} seems quite common during the early stages of tropical cyclones (e.g., Bracken and Bosart 2000; Molinari et al. 2004). Possibly as a result, both direct and indirect evidence of multiple lower-tropospheric vortices have been provided by several researchers (Ritchie and Holland 1997; Simpson et al. 1997; Davis and Bosart 2001; Ritchie et al. 2003; Hendricks et al. 2004; Molinari et al. 2004). It is likely that both wind shear and vortex interactions play a critical role in the development of many if not most tropical cyclones. The key question is how storms evolve from the sheared, asymmetric early stages to hurricane intensity. Molinari et al. (2004) argued that a sustained hurricane can develop by two processes: (i) competition among vortices produces a single near-axisymmetric vortex on the ocean surface and (ii) vertical mixing of moist entropy by convection creates a nearly slantwise neutral sounding. The incipient hurricane then satisfies the requirements of the wind-induced surface heat exchange (WISHE) instability of Emanuel (1989, 1997). By this reasoning, Gabrielle did not develop into a hurricane, even though the mesovortex central pressure was low enough to be hurricane intensity, because it remained too asymmetric (see Figs. 7–9) and, based on the lightning frequency, far from convectively neutral. One key factor in the asymmetry was the presence of very dry air upshear of the center in the lower troposphere that appeared to be drawn into the storm as it intensified. This dry air helped to prevent the tight coupling of ocean fluxes, convection, and wind needed to produce a hurricane in the WISHE theory. The lack of axisymmetry in Gabrielle compared to Hurricane Danny (1997) might reflect the 50% larger vertical wind shear in Gabrielle. Hurricane Danny contained vertical shear near 8 m s^{-1}, and a downshear vortex was able to subsequently intensify to hurricane strength (Molinari et al. 2004).

These somewhat speculative arguments do not describe the details of the formation process. Reasor et al. (2004) portrayed the complex set of possible outcomes resulting from purely dynamical interactions of vortices in the horizontal and vertical. Thermodynamic aspects, especially the influence of azimuthal moisture variation and the specific role of surface heat and moisture fluxes, are less well observed and probably less well understood than the dynamic aspects. A great deal more study is needed to untangle these processes during the early stages of tropical cyclone formation.

Finally, it is noted that vertical wind shear not only influenced the intensity of Tropical Storm Gabrielle in this study, but also the track, in that the reformed center was closer to land. The skill of Tropical Prediction Center hurricane forecasters is well known, yet at 0300 UTC 14 September, only 9 h before landfall, their landfall prediction time of 0000 UTC 15 September was 12 h too late. The effects of vertical wind shear in Gabri-

elle thus produced a storm that was both more intense and struck land much sooner than anticipated. The potential for such an outcome shows the importance of understanding the influence of vertical wind shear in storms approaching landfall.

Acknowledgments. We are indebted to several hurricane forecasters from the Tropical Prediction Center for suggesting that Tropical Storm Gabrielle might be a good case for the study of downshear reformation. The Air Force reconnaissance data were retrieved from the archive maintained by John Knaff at the Cooperative Institute for Research in the Atmosphere (CIRA); we appreciate his efforts in maintaining the archive. In addition, we express our appreciation for the dedication of the U.S. Air Force reserve personnel in repeatedly searching for the center of the storm and often flying through the most intense convection. In the process they created an outstanding data set in Tropical Storm Gabrielle (and for our previous study of Hurricane Danny). Analyses from the ECMWF were obtained from the National Center for Atmospheric Research, which is supported by the National Science Foundation. This work was supported by NASA Grant NAG511008 in association with the CAMEX-4 field experiment, and by National Science Foundation Grant ATM-0201752.

REFERENCES

Baker, M. B., A. M. Blyth, H. J. Christian, J. Latham, K. Miller, and A. M. Gadian, 1999: Relationships between lightning activity and various thundercloud parameters: Satellite and modelling studies. *Atmos. Res.,* **51,** 221–236.

Black, M. L., J. F. Gamache, F. D. Marks, C. E. Samsury, and H. E. Willoughby, 2002: Eastern Pacific Hurricanes Jimena of 1991 and Olivia of 1994: The effects of vertical shear on structure and intensity. *Mon. Wea. Rev.,* **130,** 2291–2312.

Black, R. A., and J. Hallett, 1999: Electrification of the hurricane. *J. Atmos. Sci.,* **56,** 2004–2028.

Bosart, L. F., and J. A. Bartlo, 1991: Tropical storm formation in a baroclinic environment. *Mon. Wea. Rev.,* **119,** 1979–2013.

——, C. S. Velden, W. E. Bracken, J. Molinari, and P. G. Black, 2000: Environmental influences on the rapid intensification of Hurricane Opal (1995) over the Gulf of Mexico. *Mon. Wea. Rev.,* **128,** 322–352.

Bracken, W. E., and L. F. Bosart, 2000: The role of synoptic-scale flow during tropical cyclogenesis over the North Atlantic Ocean. *Mon. Wea. Rev.,* **128,** 353–376.

Braun, S. A., 2002: A cloud-resolving simulation of Hurricane Bob (1991): Storm structure and eyewall buoyancy. *Mon. Wea. Rev.,* **130,** 1573–1592.

Cecil, D. J., and E. J. Zipser, 2002: Reflectivity, ice scattering, and lightning characteristics of hurricane eyewalls and rainbands. Part II: Intercomparison of observations. *Mon. Wea. Rev.,* **130,** 785–801.

Corbosiero, K. L., and J. Molinari, 2002: The effects of vertical wind shear on the distribution of convection in tropical cyclones. *Mon. Wea. Rev.,* **130,** 2110–2123.

——, and ——, 2003: The relationship between storm motion, vertical wind shear, and convective asymmetries in tropical cyclones. *J. Atmos. Sci.,* **60,** 366–376.

Crum, T. D., R. L. Alberty, and D. W. Burgess, 1993: Recording, archiving, and using WSR-88D data. *Bull. Amer. Meteor. Soc.,* **74,** 645–653.

Cummins, K. L., M. J. Murphy, E. A. Bardo, W. L. Hiscox, R. B. Pyle, and A. E. Pifer, 1998: A combined TOA/MDF technology upgrade of the U.S. National Lightning Detection Network. *J. Geophys. Res.,* **103,** 9035–9044.

Davis, C. A., and L. F. Bosart, 2001: Numerical simulations of the genesis of Hurricane Diana (1984). Part I: Control simulation. *Mon. Wea. Rev.,* **129,** 1859–1881.

——, and ——, 2002: Numerical simulations of the genesis of Hurricane Diana (1984). Part II: Sensitivity of track and intensity prediction. *Mon. Wea. Rev.,* **130,** 1100–1124.

——, and ——, 2003: Baroclinically induced tropical cyclogenesis. *Mon. Wea. Rev.,* **131,** 2730–2747.

DeMaria, M., 1996: The effect of vertical shear on tropical cyclone intensity change. *J. Atmos. Sci.,* **53,** 2076–2087.

——, and J. Kaplan, 1994: A statistical hurricane intensity predictions scheme (SHIPS) for the Atlantic Basin. *Wea. Forecasting,* **9,** 209–220.

——, M. Mainelli, L. K. Shay, J. A. Knaff, and J. Kaplan, 2005: Further improvements in the Statistical Hurricane Intensity Prediction Scheme (SHIPS). *Wea. Forecasting,* **20,** 531–543.

Eastin, M. D., P. G. Black, and W. M. Gray, 2002: Flight-level thermodynamic instrument wetting errors in hurricanes. Part I: Observations. *Mon. Wea. Rev.,* **130,** 825–841.

Emanuel, K. A., 1989: The finite-amplitude nature of tropical cyclogenesis. *J. Atmos. Sci.,* **46,** 3431–3456.

——, 1997: Some aspects of inner-core dynamics and energetics. *J. Atmos. Sci.,* **54,** 1014–1026.

——, C. DesAutels, C. Holloway, and R. Korte, 2004: Environmental control of tropical cyclone intensity. *J. Atmos. Sci.,* **61,** 843–858.

Enagonio, J., and M. T. Montgomery, 2001: Tropical cyclogenesis via convectively forced vortex Rossby waves in a shallow water primitive equation model. *J. Atmos. Sci.,* **58,** 685–705.

Frank, W. M., and E. A. Ritchie, 2001: Effects of vertical wind shear on the intensity and structure of numerically simulated hurricanes. *Mon. Wea. Rev.,* **129,** 2249–2269.

Franklin, J. L., S. J. Lord, S. E. Feuer, and F. D. Marks Jr., 1993: The kinematic structure of Hurricane Gloria (1985) determined from nested analyses of dropwindsonde and Doppler wind data. *Mon. Wea. Rev.,* **121,** 2433–2451.

——, M. L. Black, and K. Valde, 2003: GPS dropwindsonde wind profiles in hurricanes and their operational implications. *Wea. Forecasting,* **18,** 32–44.

Gray, W. M., 1968: Global view of the origin and tropical disturbances and storms. *Mon. Wea. Rev.,* **96,** 669–700.

Guinn, T. A., and W. H. Schubert, 1993: Hurricane spiral bands. *J. Atmos. Sci.*, **50,** 3380–3403.

Hanley, D., J. Molinari, and D. Keyser, 2001: A composite study of the interactions between tropical cyclones and upper-tropospheric troughs. *Mon. Wea. Rev.,* **129,** 2570–2584.

Hendricks, E. A., M. T. Montgomery, and C. A. Davis, 2004: The role of "vortical" hot towers in the formation of Tropical Cyclone Diana (1984). *J. Atmos. Sci.,* **61,** 1209–1232.

Heymsfield, G. M., J. Halverson, E. Ritchie, J. Simpson, J. Molinari, and L. Tian, 2006: Structure of the highly sheared Tropical Storm Chantal during CAMEX-4. *J. Atmos. Sci.,* **63,** 268–287.

Hoskins, B. J., 1990: Theory of extratropical cyclones. *Extratropical Cyclones: The Erik Palmén Memorial Volume,* C. W. Newton and E. O. Holopainen, Eds., Amer. Meteor. Soc., 64–80.

Idone, V. P., D. A. Davis, P. K. Moore, Y. Wang, R. W. Henderson, M. Ries, and P. F. Jamason, 1998a: Performance evaluation of the National Lightning Detection Network in eastern New York. 1: Detection efficiency. *J. Geophys. Res.,* **103,** 9045–9055.

——, ——, ——, ——, ——, ——, and ——, 1998b: Performance evaluation of the National Lightning Detection Network in eastern New York. 2: Location accuracy. *J. Geophys. Res.,* **103,** 9057–9069.

Knupp, K. R., J. Walters, and M. Biggerstaff, 2006: Doppler profiler and radar observations of boundary layer variability during the landfall of Tropical Storm Gabrielle. *J. Atmos. Sci.,* **63,** 234–251.

Lawrence, M., and R. Blake, 2002: Preliminary Report: Hurricane Danny 16–26 July 1997. National Hurricane Center, 18 pp. [Available online at http://www.nhc.noaa.gov/.]

Marks, F. D., Jr., R. A. Houze Jr., and J. F. Gamache, 1992: Dual-aircraft investigation of the inner core of Hurricane Norbert. Part I: Kinematic structure. *J. Atmos. Sci.,* **49,** 919–942.

Molinari, J., and D. Vollaro, 1989: External influences on hurricane intensity. Part I: Outflow layer eddy angular momentum fluxes. *J. Atmos. Sci.,* **46,** 1093–1105.

——, and ——, 1990: External influences on hurricane intensity. Part II: Vertical structure and response of the hurricane vortex. *J. Atmos. Sci.,* **47,** 1902–1918.

——, S. Skubis, and D. Vollaro, 1995: External influences on hurricane intensity. Part III: Potential vorticity structure. *J. Atmos. Sci.,* **52,** 3593–3606.

——, ——, ——, F. Alsheimer, and H. Willoughby, 1998: Potential vorticity analysis of hurricane intensification. *J. Atmos. Sci.,* **55,** 2632–2644.

——, P. Moore, and V. Idone, 1999: Convective structure of hurricanes as revealed by lightning locations. *Mon. Wea. Rev.,* **127,** 520–534.

——, D. Vollaro, and K. L. Corbosiero, 2004: Tropical cyclone formation in a sheared environment: A case study. *J. Atmos. Sci.*, **61,** 2493–2509.

Möller, J. D., and M. T. Montgomery, 2000: Tropical cyclone evolution via potential vorticity anomalies in a three-dimensional balance model. *J. Atmos. Sci.,* **57,** 3366–3387.

Montgomery, M. T., and J. Enagonio, 1998: Tropical cyclogenesis via convectively forced vortex Rossby waves in a three-dimensional quasigeostrophic model. *J. Atmos. Sci.,* **55,** 3176–3207.

Musgrave, K., C. A. Davis, and M. T. Montgomery, 2004: The effects of vertical wind shear on the formation of Hurricane Gabrielle (2001). Preprints, *26th Conf. on Hurricanes and Tropical Meteorology,* Miami Beach, FL, Amer. Meteor. Soc., 42–43.

Orville, R. E., 1991: Calibration of a magnetic direction finding network using measured triggered lightning return stroke peak currents. *J. Geophys. Res.,* **96,** 17 135–17 142.

Raymond, D. J., 1992: Nonlinear balance and potential vorticity thinking at large Rossby number. *Quart. J. Roy. Meteor. Soc.,* **118,** 987–1016.

Reasor, P. D., and M. T. Montgomery, 2001: Three-dimensional alignment and corotation of weak, TC-like vortices via linear vortex Rossby waves. *J. Atmos. Sci.,* **58,** 2306–2330.

——, ——, F. D. Marks Jr., and J. F. Gamache, 2000: Low-wavenumber structure and evolution of the hurricane inner core observed by airborne dual-Doppler radar. *Mon. Wea. Rev.,* **128,** 1653–1680.

——, ——, and L. D. Grasso, 2004: A new look at the problem of tropical cyclones in vertical shear flow: Vortex resiliency. *J. Atmos. Sci.,* **61,** 3–22.

Ritchie, E. A., and G. J. Holland, 1997: Scale interactions during the formation of Typhoon Irving. *Mon. Wea. Rev.,* **125,** 1377–1396.

——, J. Simpson, W. T. Liu, J. Halverson, C. Velden, K. F. Brueske, and H. Pierce, 2003: Present-day satellite technology for hurricane research: A closer look at formation and intensification. *Hurricane! Coping with Disaster,* R. Simpson, Ed., Amer. Geophys. Union, 249–290.

Shi, J.-J., S. W.-J. Chang, and S. Raman, 1997: Interaction between Hurricane Florence (1988) and an upper-tropospheric westerly trough. *J. Atmos. Sci.,* **54,** 1231–1247.

Simpson, J., E. Ritchie, G. J. Holland, J. Halverson, and S. Stewart, 1997: Mesoscale interactions in tropical cyclone genesis. *Mon. Wea. Rev.,* **125,** 2643–2661.

Thorpe, A. J., 1986: Synoptic scale disturbances with circular symmetry. *Mon. Wea. Rev.,* **114,** 1384–1389.

Trier, S. B., C. A. Davis, and J. D. Tuttle, 2000a: Long-lived mesoconvective vortices and their environment. Part I: Observations from the central United States during the 1998 warm season. *Mon. Wea. Rev.,* **128,** 3376–3395.

——, ——, and W. C. Skamarock, 2000b: Long-lived mesoconvective vortices and their environment. Part II: Induced thermodynamic destabilization in idealized simulations. *Mon. Wea. Rev.,* **128,** 3396–3412.

Wang, Y., and G. J. Holland, 1996: Tropical cyclone motion and evolution in vertical shear. *J. Atmos. Sci.,* **53,** 3313–3332.

Willoughby, H. E., F. D. Marks Jr., and R. J. Feinberg, 1984: Stationary and moving convective bands in hurricanes. *J. Atmos. Sci.,* **41,** 3189–3211.

Zehr, R. M., 1992: Tropical cyclogenesis in the western North Pacific. NOAA Tech. Rep. 61, 181 pp.

Zipser, E. J., and K. R. Lutz, 1994: The vertical profile of radar reflectivity of convective cells: A strong indicator of storm intensity and lightning probability? *Mon. Wea. Rev.,* **122,** 1751–1759.